Optical and structural study of GaN nanowires grown by catalyst-free molecular beam epitaxy. II. Sub-band-gap luminescence and electron irradiation effects

Lawrence H. Robins[a)]
National Institute of Standards and Technology, Gaithersburg, Maryland 20899

Kris A. Bertness, Joy M. Barker, Norman A. Sanford, and John B. Schlager
National Institute of Standards and Technology, Boulder, Colorado 80305

(Received 9 May 2006; accepted 28 March 2007; published online 4 June 2007)

GaN nanowires with diameters of 50–250 nm, grown by catalyst-free molecular beam epitaxy, were characterized by photoluminescence (PL) and cathodoluminescence (CL) spectroscopy at temperatures from 3 to 297 K. Both as-grown samples and dispersions of the nanowires onto other substrates were examined. The properties of the near-band-edge PL and CL spectra were discussed in Part I of this study by [Robins *et al.* [L. H. Robins, K. A. Bertness, J. M. Barker, N. A. Sanford, and J. B. Schlager, J. Appl. Phys. **101**,113505 (2007)]. Spectral features below the band gap, and the effect of extended electron irradiation on the CL, are discussed in Part II. The observed sub-band-gap PL and CL peaks are identified as phonon replicas of the free-exciton transitions, or excitons bound to structural defects or surface states. The defect-related peaks in the nanowires are correlated with luminescence lines previously reported in GaN films, denoted the *Y* lines [M. A. Reshchikov and H. Morkoc, J. Appl. Phys. **97**, 061301 (2005)]. The CL was partially quenched by electron beam irradiation for an extended time; the quenching was stronger for the free and shallow-donor-bound exciton peaks than for the defect-related peaks. The quenching appeared to saturate at high irradiation dose (with final intensity ≈30% of initial intensity) and was reversible on thermal cycling to room temperature. The electron irradiation-induced quenching of the CL is ascribed to charge injection and trapping phenomena.

I. INTRODUCTION

The optical properties of GaN nanowires[1] and related quasi-one-dimensional structures are of great current interest because of the potential applications in light-emitting diodes,[2,3] laser diodes,[4] and other photonic devices. We have performed a spectroscopic photoluminescence (PL) and cathodoluminescence (CL) study of GaN nanowires grown on Si(111) substrates by catalyst-free, nitrogen-plasma-assisted molecular beam epitaxy (MBE). MBE is an attractive growth technology[5–7] for GaN-based nanophotonic devices that require material with low impurity and defect content. In a companion article[8] (Part I of this study), PL and CL peaks in the near-band-edge region were examined, and the line shapes of these peaks were discussed. In this paper (Part II), PL and CL peaks in the sub-band-gap region (approximately 3.15 to 3.45 eV) are examined. In addition, the effect of extended electron irradiation on the CL is investigated. Finally, we compare our results with previous PL and CL studies of GaN nanowires, and with a review[9] of defect-related luminescence in GaN.

II. EXPERIMENTAL PROCEDURE

Procedures for MBE nanowire growth, preparation of dispersed samples (consisting of separated individual nanowires, or small clusters, on substrates other than the growth substrate), and structural and optical characterization, were described in Part I of this study[8] and previous[10–12] publications. The samples examined in this study are designated[10,11] samples B724 and B738. Some key features of the experimental procedure are restated here. PL spectra were obtained with the sample mounted on the cold finger of a variable-temperature liquid-He cryostat, with temperature control from 3 to 297 K. PL was excited by a 325.03 nm (3.813 eV) HeCd laser, with incident intensity of $\approx 3\times 10^3$ W/cm^2 for measurements of the as-grown samples and B724 dispersed on sapphire, and incident intensity of 85 W/cm^2 for measurements of B738 dispersed on sapphire. CL spectra were obtained at ≈15 K or 297 K with the sample mounted on a liquid-He cold stage in a LaB_6 filament scanning electron microscope (SEM). The peak excitation intensity for CL (the ratio of excitation power to focused beam spot size) was 9×10^3 to 3×10^4 W/cm^2, and the time-averaged excitation intensity was 0.19 to 2.4 W/cm^2. For both PL and CL, the photon energy calibration was established using atomic spectral lines. The energy calibration uncertainty was $\pm 5\times 10^{-4}$ eV for PL, and $\pm 1.6\times 10^{-5}E^2$ eV (where E is photon energy in eV) for CL.

III. RESULTS

Low-temperature PL and CL spectra from the nanowire samples are plotted in Figs. 1 and 2. PL spectra from an as-grown piece of B724 ($T=10$ K, short dashes), a polished (matrix layer+nanowire roots) piece ($T=3$ K, dash-dotted),

[a)]Electronic mail: lawrence.robins@nist.gov

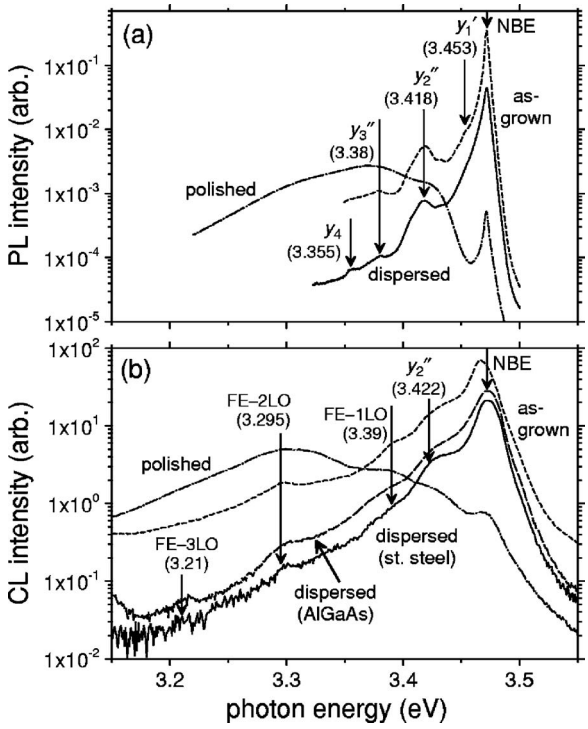

FIG. 1. Low-temperature PL and CL spectra of as-grown, dispersed, and polished pieces of sample B724. The near-band-edge (NBE) peak at ≈3.472 eV and several lower-energy peaks are indicated by vertical arrows. Each peak is labeled by name and estimated energy. (a) PL spectra of as-grown piece at $T=10$ K (short dashes), dispersed nanowires on sapphire at 10 K (solid line), and polished (matrix layer+nanowire roots) piece at 3 K (dash-dotted). (b) CL spectra (at $T\approx 15$ K) of as-grown piece (short dashes), dispersed nanowires on stainless steel (solid line), dispersed nanowires on AlGaAs (long dashes), and polished piece (dash-dotted). The CL intensities for the dispersed nanowires on stainless steel and on AlGaAs were multiplied by factors of 10 and 2, respectively, for ease of comparison.

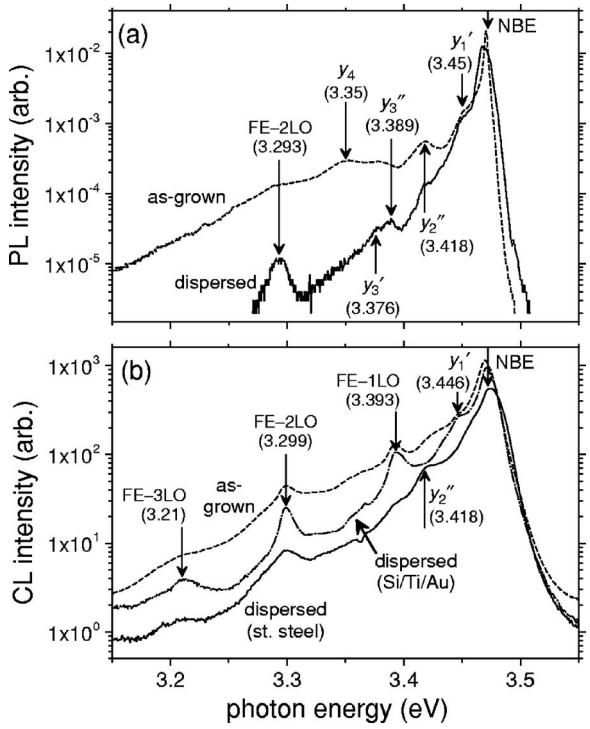

FIG. 2. Low-temperature PL and CL spectra of as-grown and dispersed pieces of sample B738. The near-band-edge (NBE) peak at ≈3.472 eV and several lower-energy peaks are indicated by vertical arrows. Each peak is labeled by name and estimated energy (in eV). (a) PL spectra (at $T=10$ K) of as-grown piece (short dashes) and dispersed nanowires on sapphire (solid line). (b) CL spectra (at $T\approx 15$ K) of as-grown piece (short dashes), dispersed nanowires on stainless steel (solid line), and dispersed nanowires on Si/Ti/Au (dash-dotted). The CL intensities for the dispersed nanowires on stainless steel and on Si/Ti/Au were multiplied by factors of 62.5 and 100, respectively, for ease of comparison.

and a dispersion on sapphire ($T=10$ K, solid line) are shown in Fig. 1(a). CL spectra taken at ≈15 K from an as-grown piece of B724 (short dashes), a polished piece (dash-dotted), a dispersion on stainless steel (solid line), and a dispersion on AlGaAs/GaAs (long dashes) are shown in Fig. 1(b). PL spectra from an as-grown piece of B738 ($T=10$ K, short dashes) and a dispersion on sapphire ($T=3.7$ K, solid line) are shown in Fig. 2(a). CL spectra taken at ≈15 K from an as-grown piece of B738 (short dashes), a dispersion on stainless steel (solid line), and a dispersion on Si/Ti/Au (dash-dotted), and a single, straight nanowire from a dispersion on Si/Ti/Au (long dashes) are shown in Fig. 2(b).

The near-band-edge (NBE) luminescence peak, indicated by vertical arrows at 3.472 eV in Figs. 1 and 2, is ascribed (at low temperature) primarily to A excitons bound to neutral, shallow donor impurities,[9] denoted D^0X_A. Properties of the NBE peak were discussed in Part I of this study. Peaks at lower energy than the NBE peak are tentatively ascribed to phonon replicas of the free-exciton transitions (designated FE–1LO, FE–2LO, and FE–3LO), and to defect-related "Y lines" that were previously reported in GaN films[9] or nanowires.[5] The defect-related lines in the nanowires in this study are designated by lower-case symbols, y_1 to y_4, to indicate a tentative correlation with the Y_1 to Y_4 lines previously reported in the literature. It should be pointed out that, in PL spectra of single nanowires with good morphology[13] (straight, unbranched wires of uniform diameter), the one-phonon to three-phonon replica lines were observed, but y lines were not observed.

According to Ref. 9, each of the Y_1 to Y_4 lines (or "groups") consist of two components (or "subgroups") separated by ≈0.01 eV, which are labeled by single-prime ($\prime$) and double-prime ($\prime\prime$) symbols in order of increasing energy (e.g., the Y_1 group consists of the Y_1' subgroup at 3.45 eV and the Y_1'' subgroup at 3.46 eV). We adapt the convention of labeling the y lines in the nanowires with ($\prime$) or ($\prime\prime$) symbols, where possible, to indicate correlation with the lower-energy or higher-energy subgroups. In Figs. 1 and 2, each peak is marked by a vertical arrow, and labeled with the estimated peak energy and designation: e.g., NBE for near-band-edge, FE–1LO for the free-exciton one-phonon replica, y_1' for a defect-related peak.

The NBE peak is seen to be the most intense component of the PL and CL spectra of all as-grown or dispersed samples. On the other hand, broad sub-band-gap (3.2–3.45 eV) peaks are the most intense components of the spectra of the polished piece of B724 [shown in Figs. 1(a) and 1(b)]. In addition, the intensity ratios of the sub-band-gap peaks to the NBE peak are larger in the as-grown samples, which contain both nanowires and matrix layer, than in the dispersed samples, which contain primarily the upper portions of the

TABLE I. Names, emission energies, and descriptions of sub-band-gap luminescence peaks in GaN nanowires (this study) and films (Ref. 9). Column 1: peak names and emission energies (or energy ranges), this study. Column 2: Names and emission energies, free or shallow-donor-bound exciton transitions in films (see Table I of Ref. 9). Column 3: Names and emission energies, *Y* defect lines in films (see Table V of Ref. 9). Column 4: tentative models for *Y* lines in films.

Peak name and energy (this study)	Free or donor-bound exciton lines in GaN films	*Y* lines in GaN films	Tentative structural model for *Y* line
y_1' (3.446–3.453 eV)	Donor-bound exciton, two-electron satellites (3.44–3.46 eV)	Y_1' (3.45 eV)	Inversion domain interface in bulk
		Y_1'' (3.46 eV)	
y_2'' (3.418–3.422 eV)		Y_2' (3.41 eV)	Surface defect, specific structure not known
		Y_2'' (3.42 eV)	
FE–1LO (3.390–3.393 eV)	FE–1LO (3.387 eV)		
y_3' (3.373–3.376 eV)		Y_3' (3.37 eV)	No model proposed
y_3'' (3.385–3.389 eV)		Y_3'' (3.38 eV)	
y_4' (3.353 eV)		Y_4' (3.35 eV)	Edge dislocation intersecting surface
y_4'' (3.366 eV)		Y_4'' (3.362 eV)	
		Y_5 (3.34 eV)	No model proposed
FE–2LO (3.293–3.299 eV)	FE–2LO (3.295 eV)	Y_6 (3.32 eV)	Donor-acceptor pair on surface
FE–3LO (≈3.21 eV)		Y_7' (3.21 eV)	Edge dislocation in bulk
		Y_7'' (3.23 eV)	

nanowires. The latter observation is not surprising, because the of the dominant contribution of the sub-band-gap peaks in the PL and CL spectra of the matrix layer (seen in the polished piece of B724).

Some additional observations about the sub-band-gap peaks are as follows. The free-exciton phonon replica peaks are stronger in CL than PL, and are particularly well-resolved in the CL spectra of the as-grown piece and dispersed on Si/Ti/Au piece of sample B738 [Fig. 2(b)]. The y_2'' peak is the most intense defect-related peak, and occurs in both PL and CL spectra. Weak y_3 group peaks occur in PL spectra, but are not observed (or not resolved from the background) in CL. Weak y_4 group peaks occur in PL spectra, and in CL spectra of sample B738 (see the discussion of electron irradiation effects).

The energies of the sub-band-gap (3.15 to 3.45 eV) peaks in the GaN nanowires in this study, and related lines previously observed in GaN films, are listed in Table I. The first column of Table I shows the names and emission energies of the peaks in the nanowires; the second column shows lines ascribed to free or shallow-donor-bound exciton transitions in films (from Table I of Ref. 9); and the third column shows the *Y* lines in films (from Table V of Ref. 9). For completeness, lines Y_1 to Y_7 are listed in the third column of Table I, although only peaks correlated with Y_1 to Y_4 were identified in the nanowires. The fourth column gives tentative structural models for the *Y* lines, as discussed in Ref. 9.

The broad "blue" and "yellow" luminescence bands (at lower emission energies than displayed in Figs. 1 and 2), which have been observed[9] in many thin-film and bulklike GaN samples, were not detectable in PL spectra of single, straight nanowires from the dispersed pieces of B724 and B738. For PL measurements that included the visible spectral range, the excitation intensity was approximately 400 W/cm^2, and the ratio of the noise level to the intensity of the NBE peak was approximately 5×10^{-4} to 10^{-3}. In several CL measurements of dispersed pieces in the 2.6 to 3.6 eV range, with peak excitation intensity of 9×10^3 to 3×10^4 W/cm^2 and time-averaged (over the raster scan period) excitation intensity of 0.19 to 2.4 W/cm^2, a weak "blue" band was observed at ≈2.9 eV, with intensity ratio to the NBE peak of 2×10^{-3} to 4×10^{-3}. The CL spectra in this study were taken from relatively large sample areas, at least 50×50 μm. Hence, the blue band may arise partially or entirely from the contribution of matrix layer material, that is known to be highly defective (spectra of polished pieces of sample B724 in Fig. 1), or from nanostructures with "branched" or "finlike" morphologies [e.g., Fig. 5 of Ref. 10 and Fig. 1(a) of Ref. 11], that are likely to contain more defects than straight nanowires.

The temperature dependencies from 3 to 100 K of PL spectra from the as-grown and dispersed pieces of sample B724, and the dispersed piece of B738, are shown in Figs. 3(a)–3(c), respectively. Temperature dependencies of the NBE features (free and shallow-donor-bound exciton peaks) were discussed[8] in Part I of this study. In Fig. 3, the intensity ratios of the y_1 to y_4 defect peaks to the broad "background" PL are seen to decrease with increasing temperature; the *y* peaks are mostly unobservable at $T\geq60$ K and completely unobservable at $T\geq100$ K. For B738 dispersed on sapphire [Fig. 3(c)], a broader peak at slightly higher energy than the y_3' or y_3'' peaks occurs at the higher temperatures; this peak is ascribed to the free-exciton one-phonon replica (FE–1LO), which is expected to show a different temperature dependence than the *y* peaks.

The CL intensity was observed to decrease with increasing electron irradiation dose. (The CL spectra shown in Figs. 1 and 2 were acquired at short irradiation times, such that the

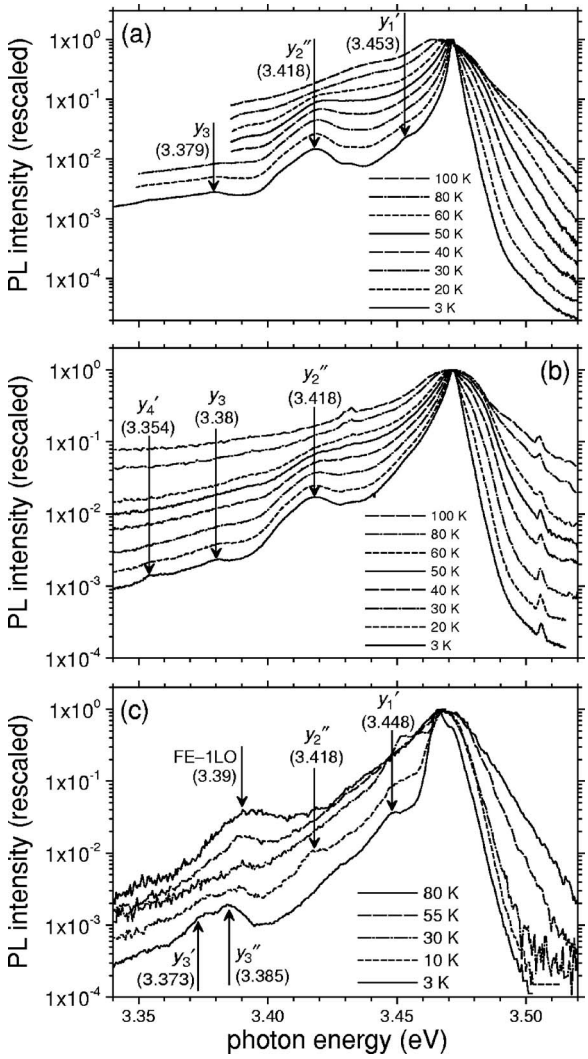

FIG. 3. Temperature dependence from 3 to 100 K of PL spectra: (a) B724, as-grown piece; (b) B724, dispersion on sapphire; (c) B738, dispersion on sapphire. The NBE peak at 3.472 eV (energy position at low temperature), y_1 to y_4 defect peaks, and free-exciton one-phonon replica (FE–1LO) peak (in B738 on sapphire) are labeled.

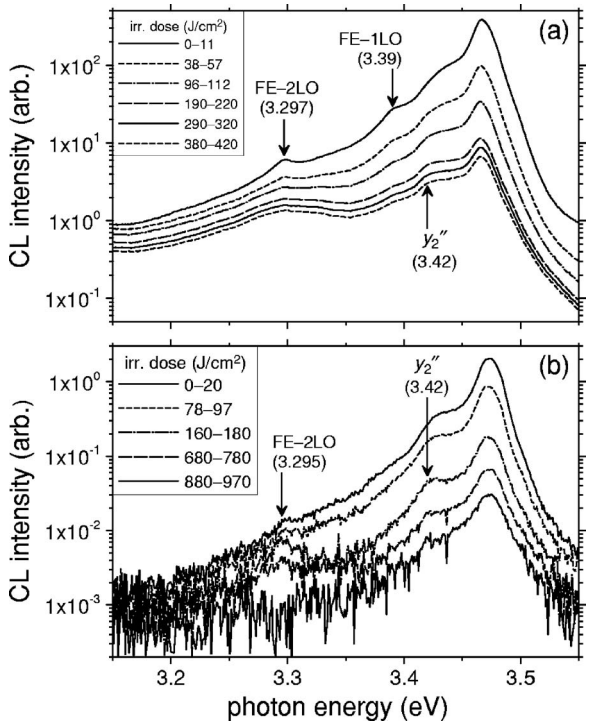

FIG. 4. Dependence of low-temperature CL spectrum on electron irradiation dose (total incident energy density, measured from the onset of electron beam irradiation, in units of J/cm^2) for sample B724: (a) as-grown; (b) dispersed on stainless steel. Defect peaks are indicated by vertical arrows and labeled with the defect name (y_1 to y_7) and peak energy.

NBE peak intensity was reduced by less than 25% from its initial value.) Electron irradiation effects on the CL spectra of selected samples are shown in Figs. 4 and 5. CL spectra acquired at different irradiation doses for the as-grown and dispersed on stainless-steel pieces of sample B724 are plotted in Figs. 4(a) and 4(b), respectively. (The irradiation dose is defined as the time-integrated incident energy density, in units of Joule/cm^2, measured from the onset of irradiation. The irradiation dose was not corrected for electron backscatter.) CL spectra acquired at different irradiation doses for the as-grown and dispersed on Si/Ti/Au pieces of sample B738 are plotted in Figs. 5(a) and 5(b), respectively. Each CL spectrum was acquired for a nonzero time interval, which corresponds to an irradiation dose range. For example, the lower spectrum in Fig. 4(a) was acquired from 1200 to 1300 s, which corresponds to irradiation doses from 380 to 420 J/cm^2. In Figs. 4 and 5, the sub-band-gap peaks are indicated by vertical arrows and labeled by name (phonon replicas FE–1LO–FE–3LO, and defect lines y_1' to y_4') and peak energy. It can be seen that the y lines were quenched less strongly by the electron irradiation than the NBE peak or the phonon replica peaks. Thus, the intensity ratios of the y lines to other spectral features show an increase with increasing irradiation dose. This trend is especially pronounced for the y_1' and y_2'' lines in the as-grown piece of sample B738 [Fig. 5(a)]; for this sample, the y_2'' line becomes more intense than then NBE peak at high irradiation dose.

A thermal cycling experiment was performed to elucidate the mechanism for the electron irradiation quenching of the CL, as follows. First, a small cluster of nanowires within sample B738 dispersed on Si/Ti/Au was irradiated at $T \approx 15$ K, and CL spectra were acquired during the irradiation process, as shown in Fig. 5(b). Second, the sample was allowed to "rest" without electron exposure for several hours at $T \approx 15$ K, and the CL was then re-examined; no recovery of the CL intensity was observed at this point. Third, the sample was warmed to $T \approx 297$ K and allowed to rest for 44 h. Finally, the sample was again cooled to ≈ 15 K, and a new electron irradiation and CL acquisition sequence was started. (Secondary electron and CL imaging verified that the same cluster of nanowires was examined throughout the experiment.) The spectrally integrated CL intensity is plotted in Fig. 6 as a function of irradiation dose and thermal cycling, with the following parameters: voltage=4.89 kV, current =8.2 nA, beam raster area 2.8×10^3 μm^2, and thus time-averaged excitation intensity of 1.4 W/cm^2.

The irradiation quenching of the CL is seen to be partly to completely reversed by cycling to room temperature. Further, the results suggest that the quenching effect saturates at high irradiation dose; i.e., the CL intensity appears to ap-

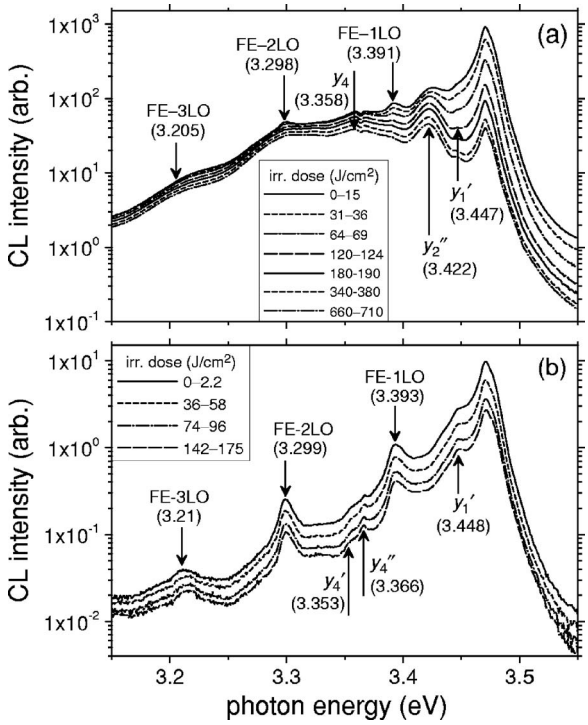

FIG. 5. Dependence of low-temperature CL spectrum on electron irradiation dose for sample B738: (a) as-grown; (b) dispersed on Si/Ti/Au. Defect peaks are indicated by vertical arrows and labeled with the defect name (y_1 to y_7) and peak energy.

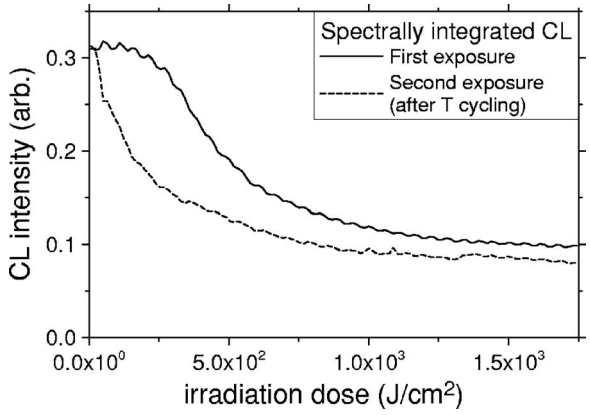

FIG. 6. Spectrally integrated CL intensity as a function of electron irradiation dose and thermal cycling for small cluster of nanowires within sample B738 dispersed on Si/Ti/Au. Solid line: irradiation quenching of CL intensity at $T \approx 15$ K during first electron-beam exposure (before thermal cycling). Dashed line: irradiation quenching of CL intensity at $T \approx 15$ K during second electron-beam exposure, after thermal cycling (44 h at room temperature). The following electron beam parameters were used: voltage =4.89 kV, current=8.2 nA, beam raster area 2.8×10^3 μm^2, and thus time-averaged excitation intensity of 1.4 W/cm^2.

proach a steady-state value of ≈30% of the initial intensity. The apparent difference between the "before thermal cycling" (solid) and "after cycling" (dashed) curves may be due to unintended zero offsets of the irradiation dose scale (x-axis in Fig. 6). In other words, some electron irradiation probably occurred before the start of data acquisition (during the optical and electron beam alignment procedure), especially in the after cycling part of the experiment.

IV. DISCUSSION

A. Correlation of sub-band-gap peaks in GaN nanowires and films

Consider first the energies of the free-exciton phonon replicas. The FE–1LO peak occurs at slightly higher energy (3.390–3.393 eV) in the nanowires than the value of 3.387 eV usually reported[9] in the literature for GaN films. The FE–2LO peak energy in the nanowires is similar to the literature value of 3.295 eV; the FE–3LO peak has not been widely reported. The small blueshift of the FE–1LO peak in the nanowires, relative to the literature value, could be due to exciton band-filling effects (i.e., phonon coupling to free excitons with energies greater than the band minimum), or strong phonon coupling to B exciton states (note that the B exciton[14] lies 5 meV higher than the A exciton in unstrained, single-crystal GaN).

As shown in Table I, the energies of the y_1' to y_4' peaks in the nanowires are in good agreement with the energies of the corresponding Y defect luminescence lines[9,15] in GaN films. Another similarity between the y lines in the nanowires and the Y lines in films is the relatively low temperature for thermally activated quenching; the y lines are mostly quenched when the temperature is increased to 60 K, and almost completely quenched by 100 K. Reshchikov[9] proposed a generalized model for the defects that give rise to the Y lines, with the basic assumption that each defect type consists of an exciton bound to a point defect or impurity, which is in turn trapped in the strain field of a bulk structural defect (e.g., dislocation, inversion domain boundary) or surface state. Within this model, the Y_2 and Y_4 lines were tentatively ascribed to exciton-point defect complexes trapped at surface states; Y_1 was tentatively ascribed to inversion domain boundaries in the bulk; a specific structural model was not proposed for Y_3.

In Table I, it can be seen that the two-electron-satellite (TES) lines[16,17] of the shallow donor-bound exciton (Fig. 7 of Ref. 16, Fig. 2 of Ref. 17) occur in the same energy range as the y_1' line in nanowires and Y_1' in films. We suggest that the y_1' line in the nanowires and Y_1' in films have a common origin, and y_1' does not arise from TES transitions, for the following reasons. First, the literature reports of well-resolved TES lines appear to be limited to thick, freestanding HVPE layers from one laboratory.[16,17] Second, both y_1' and y_2'' increase in relative intensity with electron irradiation in the as-grown piece of B738 [Fig. 5(a)], while the NBE peak (which is ascribed predominantly to shallow donor-bound excitons) decreases with electron irradiation. Finally, strong and well-resolved Y_1' and Y_1'' lines[5] were reported in a previous study of low-temperature PL and CL spectra of MBE-grown GaN nanowires.

Oil contamination related lines at 3.36 and 3.31 eV have been reported in some studies of GaN samples, and sometimes misidentified as characteristic defect lines of GaN, as discussed in Ref. 9. It is unlikely that the oil-related lines were observed in this study, for the following reasons: (a) care was taken to avoid procedures that might produce oil contamination of the samples (e.g., the CL-SEM vacuum system was based on oil-free ion, turbomolecular, and dia-

phragm pumps); (b) the 3.36 eV oil-related line (when it occurs) is often the most intense spectral feature, whereas the y_4 peaks, at energies close to 3.36 eV, were among the weakest observed features in the nanowire spectra; (c) according to Ref. 9, the oil-related lines "have often been detected in undoped GaN where no [band-edge] emission typical for GaN was observed," whereas the NBE peak was the most intense feature in the low-temperature CL and PL spectra of the nanowires.

B. Electron-irradiation-induced CL quenching

Several mechanisms could in principle induce electron irradiation quenching of the CL, including: (i) contamination by carbonaceous material that is "baked on" by the electron beam; (ii) creation of fundamental point defects such as vacancies and interstitials (which might then act as nonradiative recombination centers); or (iii) charge injection and trapping (which might then enhance the nonradiative recombination). We suggest that mechanisms (i) and (ii) can be ruled out for the following reasons. Saturation of the quenching effect at ≈30% of the initial CL intensity appears inconsistent with both (i) and (ii) (either of these mechanisms would be likely to completely quench the CL with increasing "dose"). Reversibility of the quenching at room temperature also appears inconsistent with (i) and (ii). In addition, carbonaceous contamination would be expected to expected to induce similar CL quenching effects in other luminescent materials, but we have not observed strong CL quenching in materials other than GaN nanowires (in particular, electron irradiation causes the CL intensity to increase in some materials).

A charge injection and trapping mechanism appears to be most consistent with the experimental results. Buildup of trapped charge is expected to be self-limiting (because like charges repel), which may explain the saturation; further, thermally activated release of trapped charge may explain the reversibility on thermal cycling. Finally, the enhancement of the nonradiative recombination rate by the electric fields of trapped charges is likely to be larger for delocalized or weakly localized electronic states than strongly localized states; this effect may explain the observation that the free and shallow donor-bound exciton peaks are quenched more strongly than the y defect peaks.

Campo[18] *et al.* investigated the effect of electron irradiation on room-temperature CL of GaN structures fabricated by epitaxial lateral overgrowth metal-organic chemical vapor deposition (MOCVD). In Ref. 18, the band-edge CL was reduced to 70% of its initial value after 400 s irradiation by a 20 keV, 35 nA electron beam, while the "yellow luminescence" at 500–700 nm was not reduced measurably by the irradiation. In addition, both energy-dispersive and wavelength-dispersive x-ray spectroscopy were used to search for carbon contamination of the electron-irradiated GaN surfaces; no carbon was detected by these techniques. Campo[18] *et al.* concluded that the CL quenching in their experiment was due to charge injection and trapping, as suggested in this study. Note that the vacuum system used in Ref. 18 is similar to the system in our CL setup.

C. Intensity ratios of defect luminescence peaks to near-band-edge peak

The defect-related peaks are generally lower in intensity than the NBE peak in low-temperature PL and CL spectra of the nanowires (Figs. 1, 2, 4, and 5). The only exception is the CL spectrum of the as-grown piece of sample B738 under high electron irradiation dose [Fig. 5(a)], in which the y_2'' peak is more intense than the NBE peak. The observation of low-intensity ratios of the y_1' to y_4' peaks (as well as the longer-wavelength "blue" and "yellow" bands) to the NBE peak is a qualitative indication of low defect density in the nanowires.

At low temperature, the NBE peak is ascribed primarily to excitons bound to neutral, shallow donors, as discussed[8] in Part I of this study. The donor concentration in nominally undoped GaN films, as determined by Hall effect or other electrical characterization methods, is typically[9] of the order 10^{17} cm^{-3}. Thus, the low-intensity ratios of the defect peaks to the NBE peak in the nanowires appear consistent with underlying defect concentrations of less than 10^{17} cm^{-3}. This conclusion is uncertain because of the imperfect correlation between the intensities of defect luminescence peaks and the underlying defect concentrations.

D. Comparison with previous luminescence studies of GaN nanowires

Other recent luminescence studies of GaN nanowires are briefly discussed here, classified according to the type of nanowire fabrication process. The first type of process is nitrogen-plasma-assisted MBE, as in this study. Calleja *et al.*[5] observed that the D^0X_A and X_A lines were the dominant features in low-temperature PL ($T \approx 4$ K) and CL ($T \approx 10$ K) spectra of 60–150 nm diameter, MBE-grown GaN nanowires on Si(111) and sapphire(0001). In addition, strong defect-related lines reported in Ref. 5 can be ascribed to the Y_1' and Y_1'' lines (doublet at 3.452 and 3.458 eV) and Y_2', Y_2'' (broader peak near 3.41 eV). In some spectra, the intensities of the Y_1' or Y_1'' line and the D^0X_A line were approximately equal. More recently, some of the authors of Ref. 5 reported MBE growth of 0.6 μm long nanocolumns[19] of GaN directly on Si(001) (without a III nitride buffer layer). Low-temperature ($T \approx 10$ K) PL of these nanocolumns showed a narrow, intense D^0X_A line at 3.470 eV, and a less intense Y_1' line at 3.448 eV, with no deeper (than Y_1') emissions. Growth and characterization of GaN quantum[20] disks embedded in $Al_{1-x}Ga_xN$ nanowires, by authors of Ref. 5, should also be mentioned.

Park *et al.*[6] examined the temperature and excitation intensity dependence of the PL spectra of MBE-grown vertical nanowires on Si(111), with diameter from 80 to 190 nm. PL spectra at $T = 10$ K were dominated by the D^0X_A line at 3.470–3.471 eV and X_A at 3.476–3.478 eV, with a weak Y_2 (3.41–3.42 eV) peak. In a later study, Park *et al.*[21] examined the dependence of the PL on nanowire growth time and found the best optical properties, with a narrow D^0X_A line and absence of deeper defect-related lines, at intermediate times before the nanowires started to coalesce.

Densely packed hexagonal nanorods[7] with diameter of 40–100 mm and length of ≈14 μm, were grown by MBE at the Air Force Research Laboratory (AFRL, Ohio) and characterized at the National Institute of Standards and Technology (NIST). The CL spectra ($T \approx 15$ K) of the nanorods showed a NBE peak at 3.468 eV, as well as several defect-related peaks in the energy range from the band edge to 3.0 eV. The most intense of these defect peaks were a relatively broad peak at 3.436 eV (possibly arising from overlapping Y_1 and Y_2 lines) and narrower peaks at 3.200 and 3.218 eV (possibly arising from Y_7' and Y_7'').

Thillosen *et al.*[22] compared the optical properties of GaN nanowires fabricated by a bottom-up method [MBE growth of nanocolumns on Si(111) under *N*-rich conditions] and nanowires fabricated by a top-down method [MBE growth of continuous films on Si(111) under Ga-rich conditions, followed by selective reactive ion etching to create nanocolumns from the films]. PL spectra ($T=4$ K) of single nanowires fabricated by either the top-down or bottom-up method were dominated by a D^0X_A line with peak energy of 3.473 eV, indicating virtually complete strain relaxation in both cases.

The second type of nanowire fabrication process considered here is MOVPE based, with selective etching or controlled growth of nanowires. Tiginyanu *et al.*[23] observed strong D^0X_A, X_A, and *B* free-exciton (X_B) peaks in PL spectra ($T=10$ K) of GaN nanocolumns formed by photoelectrochemical etching of MOVPE-grown films. Diaz-Guerra *et al.*[24] observed the X_A peak in CL spectra ($T=90$ K) of GaN nanocolumns formed by a similar photoelectrochemical process, although defect-related peaks in the 3.0–3.3 eV range were more intense than the X_A peak in this study. D. Wang *et al.*[25] observed strong D^0X_A and X_A emission in PL spectra ($T=77$ K) of GaN nanopillar arrays formed by plasma etching through self-organized pores in an anodic alumina etch mask. T. Wang *et al.*[26] observed a peak at 3.46 eV (358 nm) with FWHM of 0.024 eV (2.5 nm) in PL spectra ($T=10$ K) of a high-density GaN nanowire array formed by a multistep etching process through an InGaN layer (grown on top of the initial GaN layer) with self-organized holes. Hersee *et al.*[27] observed intense excitonic (3.41 eV) emission, as well as a weaker yellow band, in room temperature PL of a uniform GaN nanowire array fabricated by selective growth through a silicon nitride growth-mask layer.

The third type of nanowire fabrication process is growth by inorganic CVD or PVD, usually assisted by a metal catalyst, most commonly nickel. Low-temperature CL and PL spectra of GaN nanowires fabricated by this type of process generally showed more prominent defect-related peaks and less prominent excitonic (D^0X_A and X_A) peaks than spectra of nanowires fabricated by the other processes discussed above. In some studies, the low-temperature luminescence spectrum was completely dominated by defect peaks in the 2.75–3.25 eV range, with no spectral signature of the NBE (≈3.46–3.48 eV) emission. Such defect-dominated luminescence was observed in GaN nanowires grown by substrate-free CVD from Ga_2O_3 powder[28] and flowing NH_3; by CVD on a Ni catalyst-coated Si substrate[29] from molten Ga (or molten Ga+In) and flowing NH_3; and by thermal evaporation of GaN powder on Ni catalyst nanoparticles.[30]

There have been some reports of NBE emission in GaN nanowires grown by nickel-catalyst-assisted methods have. Ha *et al.* observed[31] a broad peak at 3.48 eV (with FWHM of ≈0.08 eV) in PL ($T=10$ K) of thin nanowires, with diameter as small as 10 nm, grown by inorganic CVD from molten GaN and flowing NH_3 on a $Ni(NO_3)_2$-coated alumina substrate. Yoo *et al.*[32] observed a peak at 3.472 eV, as well as a stronger peak at 3.437 eV, in PL ($T=10$ K) of GaN nanowires grown on Ni-coated Al_2O_3 substrates by low-pressure MOVPE; the 3.437 eV peak was tentatively ascribed to excitons bound to nickel-related deep acceptor centers. Oh *et al.*[33] examined the temperature dependence of the PL of GaN nanowires grown by inorganic ($GaCl_3+NH_3$) CVD on nickel-coated sapphire substrates. Oh *et al.*[33] found that in their nanowires, at $T=10$ K, the dominant component of the PL spectrum was a peak at 3.46 eV with FWHM of ≈0.035 eV, ascribed to excitons bound to unidentified acceptors; at $T \geq 150$ K, the dominant PL component was the free-exciton (X_A) peak (with the same energy as measured in high-quality bulk samples).

To summarize the literature results, the low-temperature luminescence spectra of undoped GaN nanowires fabricated by catalyst-free MBE or MOVPE (including both "bottom up" and "top down" methods) were observed to be dominated by free-exciton (X_A) and shallow-donor-bound exciton (D^0X_A) emission. On the other hand, varying results have been obtained for the low-temperature luminescence spectra of GaN nanowires fabricated by nickel-catalyst-assisted CVD or PVD, with broad defect-related peaks and no exciton emission reported in some studies,[29,30] and strong exciton emission reported in other studies.[33]

V. CONCLUSIONS

Radiative recombination processes in as-grown and dispersed GaN nanowire samples, grown by plasma-assisted, catalyst-free MBE, were studied by low-temperature PL ($T=3$ K to $T=100$ K) and CL ($T \approx 15$ K) spectroscopy. In the 3.45–3.15 eV energy range, phonon replicas of the free-exciton (FE–1LO to FE–3LO) were observed, as well as defect peaks (denoted y_1' to y_4') correlated with defect luminescence lines previously reported in GaN films[9] (denoted Y_1' to Y_4'). It has been suggested[9] that the *Y* lines arise from excitons bound to point defects or impurities, which are in turn localized near bulk structural defects or surface states. The intensity ratios of the *y* defect peaks to the NBE peak were consistently less than unity in the low-temperature PL and CL spectra of dispersed nanowires.

The CL intensity was partially quenched by extended electron irradiation at low temperature. The CL quenching appeared to saturate (with final CL intensity ≈30% of initial intensity) at high electron irradiation dose, and the quenching was reversed by thermal cycling to room temperature. The electron irradiation-induced quenching of the CL is ascribed to charge injection and trapping phenomena.

In other studies of the optical properties of GaN nanowires fabricated by catalyst-free MBE or MOVPE methods,

the NBE peak has been found to be the most intense component of the low-temperature CL or PL spectrum. In studies of the optical properties of GaN nanowires grown by nickel-catalyst-assisted CVD or PVD, varying low-temperature luminescence results have been obtained, with broad defect-related peaks (and no NBE peak) observed in some samples, and a strong NBE peak observed in other samples.

[1]M. Law, J. Goldberger, and P. Yang, Annu. Rev. Mater. Res. **34**, 83 (2004).
[2]F. Qian, Y. Li, S. Gradecak, D. Wang, C. J. Barrelet, and C. M. Lieber, Nano Lett. **4**, 1975 (2004).
[3]F. Qian, S. Gradecak, Y. Li, C. Y. Wen, and C. M. Lieber, Nano Lett. **4**, 1975 (2004).
[4]S. Gradečak, F. Qian, Y. Li, H. G. Park, and C. M. Lieber, Appl. Phys. Lett. **87**, 173111 (2005).
[5]E. Calleja, M. A. Sanchez-Garcıa, F. J. Sanchez, F. Calle, F. B. Naranjo, E. Munoz, U. Jahn, and K. Ploog, Phys. Rev. B **62**, 16826 (2000).
[6]Y. S. Park, C. M. Park, D. J. Fu, T. W. Kang, and J. E. Oh, Appl. Phys. Lett. **85**, 5718 (2004).
[7]N. A. Sanford, L. H. Robins, M. H. Gray, Y.-S. Kang, J. E. Van Nostrand, C. Stutz, R. Cortez, A. V. Davydov, A. Shapiro, I. Levin, and A. Roshko, Phys. Status Solidi C **2**, 2357 (2005).
[8]L. H. Robins, K. A. Bertness, J. M. Barker, N. A. Sanford, and J. B. Schlager, J. Appl. Phys. **101**, 113505 (2007).
[9]M. A. Reshchikov and H. Morkoc, J. Appl. Phys. **97**, 061301 (2005).
[10]K. A. Bertness, N. A. Sanford, J. M. Barker, J. B. Schlager, A. Roshko, A. V. Davydov, and I. Levin, J. Electron. Mater. **35**, 576 (2006).
[11]K. A. Bertness, J. B. Schlager, N. A. Sanford, A. Roshko, T. E. Harvey, A. V. Davydov, I. Levin, M. D. Vaudin, J. M. Barker, P. T. Blanchard, and L. H. Robins, "High Degree of Crystalline Perfection in Spontaneously Grown GaN Nanowires," in *GaN, AlN, InN and Related Materials*, MRS Symposium Proceeding 892, edited by M. Kuball, T. H. Myers, J. M. Redwing, and T. Mukai (Materials Research Society, Warrendale, PA, 2006).
[12]K. A. Bertness, A. Roshko, N. A. Sanford, J. M. Barker, and A. V. Davydov, J. Cryst. Growth **287**, 522 (2006).
[13]J. B. Schlager, N. A. Sanford, K. A. Bertness, J. M. Barker, A. Roshko, and P. T. Blanchard, Appl. Phys. Lett. **88**, 213106 (2006).
[14]K. Torii, T. Deguchi, T. Sota, K. Suzuki, S. Chichibu, and S. Nakamura, Phys. Rev. B **60**, 4723 (1999).
[15]M. A. Reshchikov, J. Jasinski, Z. Liliental-Weber, D. Huang, L. He, P. Visconti, and H. Morkoc, Physica B (Amsterdam) **340–342**, 440 (2003).
[16]J. A. Freitas, Jr., J. Cryst. Growth **281**, 168 (2005).
[17]D. C. Look, Z. Q. Fang, and B. Claflin, J. Cryst. Growth **281**, 143 (2005).
[18]E. M. Campo, G. S. Cargill III, M. Pophristic, and I. Ferguson, MRS Internet J. Nitride Semicond. Res. **9**, 8 (2004).
[19]L. Cerutti, J. Ristic, S. Fernandez-Garrido, E. Calleja, A. Trampert, K. H. Ploog, S. Lazic, and J. M. Calleja, Appl. Phys. Lett. **88**, 213114 (2006).
[20]J. Ristić, E. Calleja, M. A. Sanchez-Garcia, J. M. Ulloa, J. Sanchez-Paramo, J. M. Calleja, U. Jahn, A. Trampert, and K. H. Ploog, Phys. Rev. B **68**, 125305 (2003).
[21]C. M. Park, Y. S. Park, H. Im, and T. W. Kang, Nanotechnology **17**, 952 (2006).
[22]N. Thillosen, K. Sebald, H. Hardtdegen, R. Meijers, R. Calarco, S. Montanari, N. Kaluza, J. Gutowski, and H. Luth, Nano Lett. **6**, 704 (2006).
[23]I. M. Tiginyanu, V. V. Ursaki, V. V. Zalamai, S. Langa, S. Hubbard, D. Pavlidis, and H. Foll, Appl. Phys. Lett. **83**, 1551 (2003).
[24]C. Díaz-Guerra, J. Piqueras, V. Popa, A. Cojocaru, and I. M. Tiginyanu, Appl. Phys. Lett. **86**, 223103 (2005).
[25]Y. D. Wang, S. J. Chua, S. Tripathy, M. S. Sander, P. Chen, and C. G. Fonstad, Appl. Phys. Lett. **86**, 071917 (2005).
[26]T. Wang, F. Ranalli, P. J. Parbrook, R. Airey, J. Bai, R. Rattlidge, and G. Hill, Appl. Phys. Lett. **86**, 103103 (2005).
[27]S. D. Hersee, X. Sun, and X. Wang, Nano Lett. **6**, 1808 (2006).
[28]T. Sekiguchi, J. Hu, and Y. Bando, J. Electron Microsc. (Tokyo) **53**, 203 (2004).
[29]L. Dai, S. F. Liu, L. P. You, J. C. Zhang, and G. G. Qin, J. Phys.: Condens. Matter **17**, L445 (2005).
[30]M. Kang, J. S. Lee, S. K. Sim, H. Kim, B. Min, K. Cho, G. T. Kim, M. Y. Sun, S. Kim, and H. S. Han, Jpn. J. Appl. Phys., Part 1 **43**, 6868 (2004).
[31]B. Ha, S. H. Seo, J. H. Cho, C. S. Yoon, J. Yoo, G. C. Yi, C. Y. Park, and C. J. Lee, J. Phys. Chem. B **109**, 11095 (2005).
[32]J. Yoo, Y. J. Hong, S. J. An, G. C. Yia, B. Chon, T. Joo, J. W. Kim, and J. S. Lee, Appl. Phys. Lett. **89**, 043124 (2006).
[33]E. Oh, J. H. Choi, H. K. Seong, and H.-J. Choi, Appl. Phys. Lett. **89**, 092109 (2006).